# NUMERICAL SIMULATIONS OF COLLAPSE AND FRAGMENTATION OF MAGNETIZED MOLECULAR CLOUD CORES — FORMATION OF BINARY SYSTEMS

Kohji Tomisaka,[1] Masahiro N. Machida,[2] Tomoaki Matsumoto,[1,3] and Kazuya Saigo[1]

RESUMEN

**El resumen será traducido al español por los editores.** The fragmentation process is studied with 3D nested grid MHD simulations. In the run-away collapse phase, the cloud contracts and forms a disk perpendicular to the local magnetic field lines, even if the initial B-field and the angular momentum are not parallel each other. Angular momentum is transferred by the magnetic field efficiently in the this phase as well as the adiabatic accretion stage afterward. The disk becomes thinner and thinner. If the oblateness (major to minor axis ratio) at the end of the run-away collapse phase is larger than 4, the disk fragments after the disk becomes adiabatic. Binary outflows are formed after the fragments contract. Another candidate for fragmentation is around the second core. Hydrodynamical simulation confirms that in the second collapse with $\gamma \simeq 1.1$ a rotation supported disk is formed, although we have no rotation supported disk during the isothermal first run-away collapse ($\gamma = 1$). Because this disk is thin, the disk is expected to fragment.

ABSTRACT

The fragmentation process is studied with 3D nested grid MHD simulations. In the run-away collapse phase, the cloud contracts and forms a disk perpendicular to the local magnetic field lines, even if the initial B-field and the angular momentum are not parallel each other. Angular momentum is transferred by the magnetic field efficiently in the this phase as well as the adiabatic accretion stage afterward. The disk becomes thinner and thinner. If the oblateness (major to minor axis ratio) at the end of the run-away collapse phase is larger than 4, the disk fragments after the disk becomes adiabatic. Binary outflows are formed after the fragments contract. Another candidate for fragmentation is around the second core. Hydrodynamical simulation confirms that in the second collapse with $\gamma \simeq 1.1$ a rotation supported disk is formed, although we have no rotation supported disk during the isothermal first run-away collapse ($\gamma = 1$). Because this disk is thin, the disk is expected to fragment.

*Key Words:* **ISM: JETS AND OUTFLOWS — MHD — STARS: BINARIES: GENERAL — STARS: FORMATION**

## 1. INTRODUCTION

Since binary and multiple stars are much more popular than the single stars, binary/multiple formation must be understood to explore the star formation process. Fragmentation is considered one of the key physical processes to understand how the binaries and multiple-star systems are formed. In this paper, we focus on the fragmentation of $m = 2$ (bar or spiral) mode, which leads to binary stars, paying attention to the effect of magnetic fields.

It is well-known that two kinds of collapse solution appear in the course of star formation. Massive cloud which is not supported against its self-gravity experiences the run-away collapse in which the central density increases greatly in a finite time-scale. After the first core is formed the contraction with accretion proceeds (Whitworth and Summers 1985). How fast does the cloud forget its initial condition and converge to the self-similar solution (Larson 1969; Penston 1969)? Ogino et al.(1999) compared the solutions with various initial $\alpha$= gravitational-to-pressure force ratios and found that the convergence depends on $\alpha$ and the cloud with $\alpha = 4$, which coincides with that of the self-similar solution, converges most quickly. It should be noted that the isothermal clouds with/without magnetic fields or rotation experience the run-away collapse (Norman et al.1980; Narita et al.1984; Tomisaka 1996). For the rotating cloud, the rotation speed at the center converges to $\Omega_c \simeq (0.3 \pm 0.1) \times (2\pi G \rho_c)^{-1/2}$ [4] irre-

[1]National Astronomical Observatory, Mitaka, Tokyo, Japan.

[2]Center for Frontier Science, Chiba University, Chiba, Japan

[3]Faculty of Humanity and Environment, Hosei University, Tokyo, Japan.

[4]The subscript c denotes the value at the center.

spective of initial conditions (Matsumoto et al.1997). While, magnetized cloud shows that the central mass-to-flux ratio converges to $2\pi G^{1/2}\sigma_c/B_c \simeq 1.0-1.5$ (Nakamura et al.1999). These facts suggest that the structure at the first-core formation is well described by a small number of parameters.

## 2. ALIGNED VS NON-ALIGNED ROTATOR

To show another example of convergence, we discuss here how the angular momentum $\mathbf{J}$ and the magnetic fields $\mathbf{B}$ become parallel each other. In the case of aligned rotator in which initial $\mathbf{J}_0$ of the cloud and $\mathbf{B}_0$ are parallel, a disk is formed in the run-away collapse phase in the direction perpendicular to $\mathbf{B}_0$ and $\mathbf{J}_0$. In this configuration, after the first core is formed gas is ejected along the magnetic field lines by the magneto-centrifugal wind mechanism (Tomisaka 1998). How about the non-aligned rotator? Figure 1 shows the difference between (a) $\theta$ =0°, (b) 45°, and (c) 90°, where $\theta$ represents the angle between $\mathbf{J}_0$ ($z$-direction) and $\mathbf{B}_0$ (Matsumoto et al.2004). In the case of $\theta = 45°$ (b), although the global $\mathbf{J}_0$ points in the $z$-direction, local $\mathbf{J}$ around the disk differs from the global one and is parallel to the direction of the local $\mathbf{B}$ which coincides with the global $\mathbf{B}_0$ in $\sim 20°$. Outflow is also ejected in the direction perpendicular to the disk or parallel to the local $\mathbf{B}$ and $\mathbf{J}$. This is valid even $\theta \lesssim 80°$. In the case of perpendicular rotator $\theta = 90°$ (c), outflow is ejected in the direction perpendicular to the global $\mathbf{J}_0$. This is similar to the magnetocentrifugal solar wind mechanism working in the rotation plane of the Solar system. In this case, a disk is formed perpendicular to the global $\mathbf{J}_0$! Except for extreme cases of $\theta \gtrsim 80°$, it is concluded that the local $\mathbf{J}$ and $\mathbf{B}$ are parallel each other when the first core is formed. The angular momentum is efficiently transferred by the magnetic field. Figure 2 shows the time evolution of specific angular momentum to mass ratio evaluated for the gas with $\rho > 0.1\rho_c$. The first core formation epoch is denoted by a diamond. This figure indicates that $\mathbf{J}$ is reduced drastically after the first core formation via the outflow. However, even in the isothermal run-away collapse phase, $\mathbf{J}$ is transferred from the contracting core.

## 3. FRAGMENTATION OF THE MAGNETIZED CLOUD

In §§1 and 2, we have shown two opposite effects of the magnetic field: encouraging formation of the pseudo disk and discouraging the disk formation via magnetic braking and thus decreasing the angular momentum. A thin disk is necessary for fragmentation, as shown later. It is not straight forward

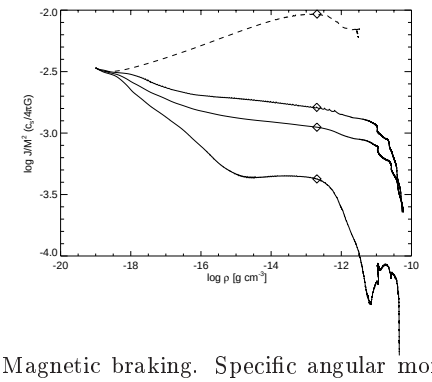


Fig. 2. Magnetic braking. Specific angular momentum to mass ratio is plotted against the central density. The cloud evolves from the left to the right. Four models are plotted: from the top to the bottom, nonmagnetic case $B_0 = 0$, $\theta = 0°$, 45°, and 90°.

whether the magnetic fields encourages the fragmentation or discourages it.

To study the non-axisymmetric evolution (binary star formation processes and the outflow), we consider a cylindrical isothermal cloud in hydrostatic balance as the initial condition. The cloud is assumed to rotate with a rotation axis which coincides with the cylindrical axis and the magnetic field lines. And the length of the cylindrical cloud $L$ is chosen equal to the wavelength of the most unstable Jeans mode acquired by the linear analysis (Matsumoto et al.1994). We chose a magneto-hydrostatic solution for the isothermal cylindrical cloud by Stodółkiewicz (1963) (for more detail, see Machida et al.2004). To begin the dynamical contraction, we added non-axisymmetric and axisymmetric density perturbations. The relative amplitude of the axisymmetric perturbation is chosen as $A_z = 0.1$. The solution has two parameters for the hydrostatic model, the magnetic to thermal pressure ratio $\alpha \equiv B_c^2/4\pi\rho_c c_s^2$ and the angular rotation speed normalized by the free-fall timescale as $\omega \equiv \Omega_c/(4\pi G\rho_c)^{1/2}$, and one parameter for the amplitude of $m = 2$ perturbation, $A_\phi = \max_{0\le\phi\le\pi}|\delta\rho/\rho|$. We use an equation of state (EOS) composed of two power-laws as isothermal EOS as $p = c_s^2\rho$ for $\rho < \rho_{\rm cr}$ while adiabatic EOS as $p = c_s^2\rho_{\rm cr}(\rho/\rho_{\rm cr})^{7/5}$ for $\rho > \rho_{\rm cr}$, in which we take $\rho_{\rm cr} = 10^{10}{\rm cm}^{-3}$ (Masunaga & Inutsuka 2000).

In the runaway collapse phase, the axisymmetric perturbation grows and forms a disk. The non-axisymmetric perturbation also grows in this isothermal run-away phase. However, fragmentation never occurs, which is defined as the density maximum appears other than the center. After reaching the density $\rho_{\rm cr}$, an adiabatic (first) core is formed and the isothermal gas outside rotates around the core and

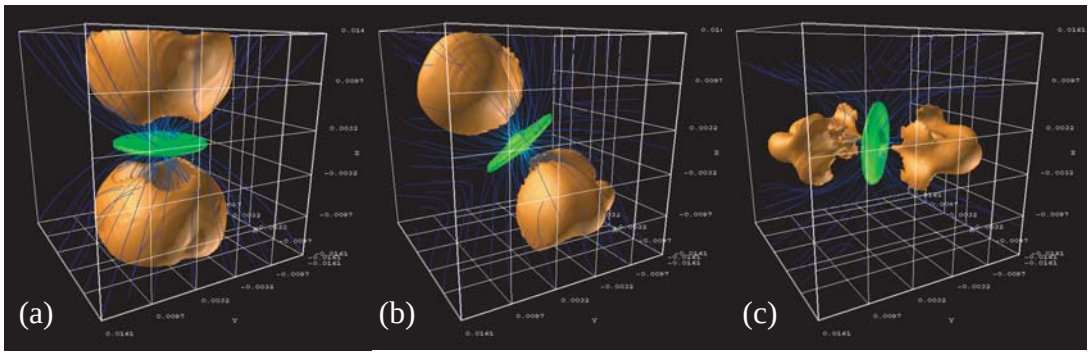


Fig. 1. Collapse of aligned (a) and non-aligned [(b) and (c)] rotating magnetized cloud. The angles between $\mathbf{J}_0$ and $\mathbf{B}_0$ are $\theta = 0°$, $45°$, and $90°$.

accretes onto it. This is the phase in which fragmentation occurs.

It is found that the evolutions are divided into three types as shown in Figure 3: **a)** (core type) in the case of slight non-axisymmetric perturbations $A_\phi \ll 1$, the adiabatic core continues to be axisymmetric. **(b)** (disk fragmentation type) in the case of weak magnetic field and fast rotation, a thin axisymmetric disk is formed in the run-away collapse. After the core formation, a spiral pattern grows in the disk and two dense cores are formed in this disk. **(c)** (bar fragmentation type) strong magnetic field transfers the angular momentum, which induces severe non-axisymmetry. Such a bar fragments into several pieces after the core formation epoch.

In Figure 4, the evolutions of the oblateness ($\epsilon_{\rm ob}$) and axis ratio ($\epsilon_{\rm ar}$) are plotted by solid lines.[5]This shows (1) the cloud forms a disk (evolution vertically upward) first and (2) non-axisymmetric pattern grows (evolution horizontally rightward) next. In this figure, the shapes of the core at the fragmentation (or at the end of simulations) are indicates by the symbols. Further, the models that experience fragmentation are denoted with crosses. This figure clearly shows that the model whose oblateness is larger than 4 ($\epsilon_{\rm ob} > 4$) seems to fragment. In other words, a thick core with $\epsilon_{\rm ob} < 4$ does not show fragmentation as in Figure 3(a). The core which reaches the region of axis ratio $\epsilon \gtrsim 4$ forms a bar and fragmentation occurs in such a cloud through the bar type (Fig.3[c]). The core thin enough $\epsilon_{\rm ob} > 4$ but slightly non-axisymmetric ($\epsilon_{\rm ar} \lesssim 4$) leads to fragmentation via the disk type in Figure 3(b).

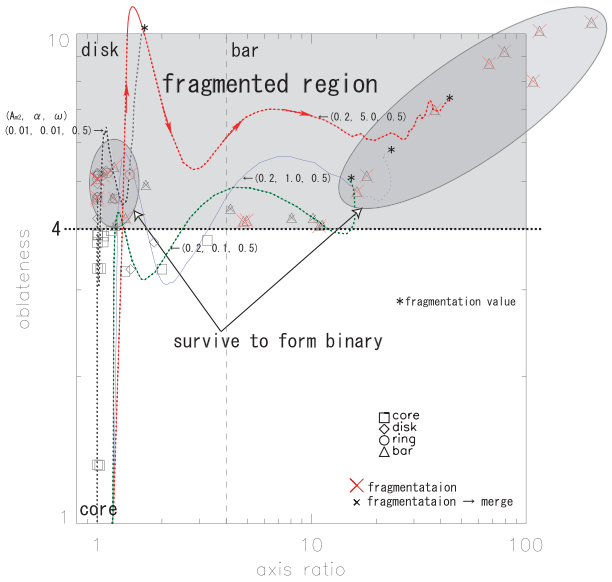


Fig. 4. The axis ratio and oblateness are plotted at the core formation epoch $\rho_c = \rho_{\rm cr}$. Cross represents a core which experiences the fragmentation. Fragmentation occurs above the horizontal dashed line ($\epsilon_{\rm ob} > 4$). The domains in large circles mean that fragmented cores survive to form binary or multiple stars. Several evolutionary tracks are plotted; solid and dotted lines represent respectively isothermal ($\rho_c < \rho_{\rm cr}$) and adiabatic phases ($\rho_c > \rho_{\rm cr}$) and asterisks indicate the point of fragmentation. The symbols □ (core), ◇ (disk), ◯ (ring) and △ (bar) denote the shape of the adiabatic core when the fragmentation occurs or the calculation ends.

## 4. FRAGMENTATION AROUND THE SECOND CORE

In §3 section, we focused on the fragmentation in the first adiabatic core. Another site of binary star formation is expected around the second core. Bate (1998) performed SPH simulations from the first runaway collapse, the first core, the second collapse, to the second core. He concluded that the second core does not fragment. However, this conclusion is strongly biased to the case in which a large part of the angular momentum seems to be transferred by strong spiral density patterns grown in the first core (Fig.3 middle panel of Bate 1998). We re-study the runaway collapse of polytropic gas with $\gamma = 1.1$

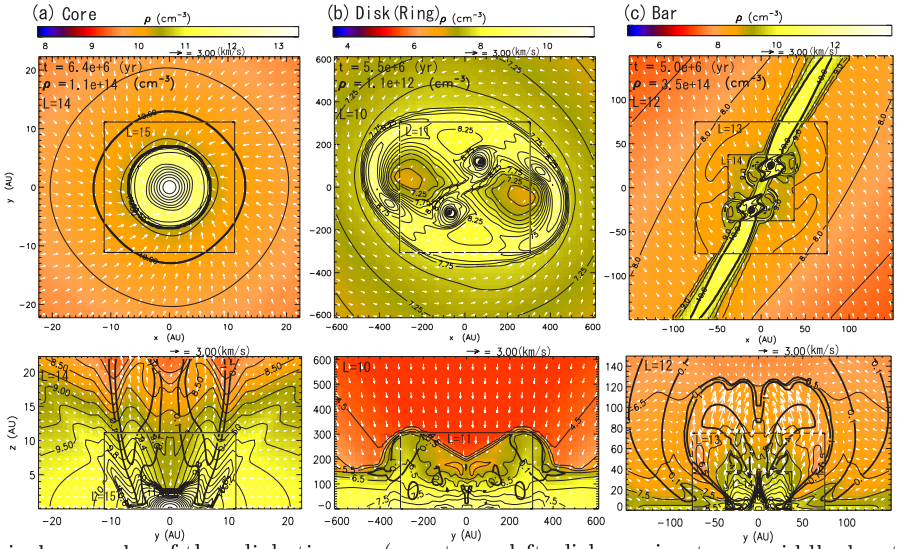


Fig. 3. Three typical examples of the adiabatic core (core-type: left, disk- or ring-type: middle, bar-type: right). Model parameters are $(A_\phi, \alpha, \omega)$ = (a): (0.0, 0.1, 0.1), (b):(0.01, 0.01, 0.5) and (c):(0.2, 1.0, 0.5). Density (contour and false color) and velocity vectors (arrows) are plotted on a plane including the major axis of the core and the $z$-axis (lower panels) and on the $z$=0 plane (upper panels). Thick lines in the upper panels denote the outline of the adiabatic core as $\rho = \rho_{\rm cr}$, while those in the lower panels mean the isovelocity curves representing the outflow region ($v_{\rm z} = 0.1, 1$ and 4 km s$^{-1}$).

which is realized in the second collapse phase induced in the first adiabatic core, using a 2D hydrocode.

As an initial setup, a hydrostatic equilibrium for rotating polytropic gas with $\gamma = 7/5$ is prepared (for more detail, see Saigo & Tomisaka 2004) using a self-consistent field method developed by Hachisu (1986). As the EOS we assume a double polytrope as $\gamma = 7/5$ for $\rho < \rho_B = 5.6 \times 10^{-9} {\rm g\,cm^{-3}}$ and $\gamma = 1.1$ for $\rho > \rho_B$. Hydrodynamical calculations show us that the angular rotation speed at the center of the first core controls the evolution. **(a)** When $\omega_c \equiv \Omega_c/(2\pi G\rho_c)^{1/2} > 0.4$ at $\rho_c \simeq 2\rho_B$, the first core does show no contraction. **(b)** If $0.3 < \omega_c < 0.4$, the second run-away collapse occurs but a rotation supported disk or a ring is made before reaching the stellar density $\rho \lesssim 10^{-3} {\rm g\,cm^{-3}}$, which is similar to Bonnell & Bate (1994). **(c)** If $\omega_c < 0.3$, the second run-away collapse proceeds to the second core. Since a thin disk is necessary for fragmentation, fragmentation seems to take place before gas density reaches the stellar density, if appropriate angular momentum is left in the first core $\omega_c > 0.3$. This is another possible occasion for the fragmentation. If the angular momentum is transferred efficiently in the first core, contraction does not stop till the second core is formed.

[5] Those are defined using the lengths of the dense core as $\rho > \rho_{\rm max}/10$. Using the length in $z$-direction, $l_z$, the major axis in the x-y plane, $l_M$, and the minor axis, $l_m$, the former is defined $(l_M l_m)^{1/2}/l_z$ and the latter is $l_M/l_m$.

Numerical calculations were carried out at ADAC-NAOJ.

## REFERENCES

Bate, M.R. 1998, ApJ, 508, L95
Bonnell, I. A. & Bate, M. R. 1994, MNRAS, 271, 999
Hachisu, I. 1986, ApJS, 61, 479
Larson, R.B. 1969, MNRAS, 145, 271
Machida, M.N., Tomisaka, K., & Matsumoto, T. 2004, MNRAS, 348, L1
Masunaga, H. & Inutsuka, S., 2000,ApJ, 531, 350
Matsumoto, T., Hanawa, T., & Nakamura, F. 1997, ApJ, 478, 569
Matsumoto, T., Machida, M.N., Tomisaka, K., & Hanawa, T. 2004, Computer Physics Communications, in press
Matsumoto, T., Nakamura, F., & Hanawa, T. 1994, PASJ, 46, 243
Nakamura, F., Matsumoto, T., Hanawa, T., & Tomisaka, K. 1999, ApJ, 510, 274
Narita, S., Hayashi, C., & Miyama, S. M. 1984, Prog. Theor. Phys. 72, 1118
Norman, M. L., Wilson, J. R., & Barton, R. T. 1980, ApJ, 239, 968
Ogino, S., Tomisaka, K., & Nakamura, F. 1999, PASJ, 51, 637
Penston, M. V. 1969, MNRAS, 145, 457
Saigo, K. & Tomisaka, K. 2004, in preparation
Stodółkiewicz, J. S. 1963, Acta Astron., 13, 30
Tomisaka, K. 1996, PASJ, 48, 701
——. 1998, ApJ, 502, 163
Whitworth, A., & Summers, D. 1985, MNRAS, 214, 1

Masahiro N. Machida: Center for Frontier Science, Chiba University, Yayoicho 1-33, Inageku, Chiba 263-8522, Japan (machida@cfs.chiba-u.ac.jp).
Tomoaki Matsumoto: Faculty of Humanity and Environment, Hosei University, Fujimi, Chiyodaku, Tokyo 102-8160, Japan (matsu@i.hosei.ac.jp).
Kazuya Saigo and Kohji Tomisaka: National Astronomical Observatory, Osawa 2-21-1, Mitaka, Tokyo 181-8588, Japan (ks,saigo@the.nao.ac.jp;kt,tomisaka@the.nao.ac.jp).